

Wavelength-switchable fiber ring laser using chirped Moiré fiber grating combined with Sagnac loop interferometer

Abstract. A simple, cost-effective and switchable five-wavelength fiber ring laser based on a chirped moiré fiber grating (CMFG) and a wavelength-tunable Sagnac loop interferometer (FSI) filter is proposed and experimentally demonstrated. To serve as wavelength selective element, the CMFG possesses excellent comb-like filtering characteristics, and its fabrication method is easy and flexible. The usage of the FSI filter helps remove the high-cost optical circulator and improve the output performance of optical signal-to-noise ratio.

Streszczenie. Zaproponowano i przedstawiono eksperymentalnie prosty, tani światłowodowy laser żyroskopowy z przełączanymi pięcioma długościami fali. Zastosowano siatkę dyfrakcyjną z efektem mory ze skompromowanego włókna (CMFG) oraz, w pętli strojenia, filtr z interferometrem z pętlą Signac'a (FSI). Wykorzystana jako element selektywny, ustalający długość fali, siatka CMFG zapewnia doskonałą, grzebieniową charakterystykę filtru, ponadto metoda jej wytwarzania jest łatwa i elastyczna. Wykorzystanie filtru FSI pomaga obniżyć koszt układu i zapewnia na wyjściu dobry stosunek sygnał/szum. **Światłowodowy laser żyroskopowy z przełączaną długością fali wykorzystujący siatkę dyfrakcyjną z efektem mory ze skompromowanego włókna w połączeniu z interferometrem z pętlą Signac'a.**

Keywords: fiber laser; chirped moiré grating; Sagnac effect

Słowa kluczowe: laser światłowodowy, skompromowana siatka dyfrakcyjna z efektem mory, efekt Signac'a

1. Introduction

Fiber lasers exhibit many attractive features such as inherent single transversal mode and compatibility with optical fiber systems. In recent years, there is a surge of interest in multi-wavelength and wavelength-switchable fiber lasers, since they are potentially useful for dense wavelength division multiplexed (DWDM) fiber communication systems, optical fiber sensor networks and instrumentation. The most important key component of these fiber lasers is a wavelength selection filter. Among versatile techniques to realize the wavelength selection filter, a fiber Bragg grating (FBG) is an ideal intra-cavity device to select the lasing wavelength, for example, the FBGs written in multimode fiber^{1,2} cascaded FBGs³⁻⁹, FBGs in Sagnac loop¹⁰, FBGs written in Hi-Bi fiber¹¹, superimposed chirped gratings^{12,13} and sampled fiber gratings^{14,15}. FBG has significant advantages such as fiber compatibility, superior spectral reflectivity and cost effectiveness. For the implementation of wavelength switching, various techniques have been used based on polarization control of the laser cavity^{1,2}, fiber loop mirror¹⁰, variable optical attenuator (VOA) between cascaded FBG segments³, control of Raman pump⁴, polarization control of high-birefringence fiber grating⁶, spectral polarization-dependent loss element⁷, amplitude modulator⁸ and optical bi-stability⁹. However, most of these methods are limited to only 2 or 3 switchable wavelengths or the switching of each single wavelength cannot be accomplished yet.

In our previous letters^{16,17}, the chirped moiré fiber grating (CMFG) is used as the wavelength selective element to realize multiwavelength and wavelength-switchable fiber lasers. The CMBG is an ideal transmissive comb filter with stable wavelength spacing, narrow filtering bandwidth and uniform channel transmittance; and it has extra advantages of easy fabrication, compactness and flexible tuning of wavelength interval within a large band depending on the chirp value.

In this letter, the chirped Moiré fiber grating (CMFG) is also chosen to help implement wavelength selection. A tunable Sagnac loop interferometer (FSI) filter is adopted to substitute the high-cost filter that contains an optical circulator. With the help of these two main components, stable wavelength-switchable lasing oscillations with wavelength spacing of about 0.25nm have been experimentally demonstrated. Due to the usage of the FSI

filter, the measured optical signal-to-noise ratio is increased from 50dB to 70dB. The power fluctuation of each wavelength is less than 0.5 dB within a one-hour period, and the output power of different channels is almost identical (difference less than 1dB) within the tunable range.

2. Theory and Fabrication of CMFG

The core refractive index of linear chirped fiber grating is described by (1)

$$(1) \quad n_{co}(z) = n_1 + \delta n \left[1 + v \cos \left(\frac{2\pi}{\Lambda} z + c \frac{z^2}{L^2} + \varphi \right) \right]$$

where n_1 is the refractive index of the fiber core before exposure, δn is the amplitude of the refractive index modulation of the Bragg grating, v is the fringe visibility of the index change, Λ is the initial period of the chirped fiber grating, c is the chirp coefficient, L is the grating length, and φ is the initial exposure phase.

When two linear chirped gratings are overlapped in the same fiber, its refractive index is (2)

$$(2) \quad n_{co}(z) = n_1 + \delta n_1 \left[1 + v_1 \cos \left(\frac{2\pi}{\Lambda_1} z + c_1 \frac{z^2}{L^2} + \varphi_1 \right) \right] + \delta n_2 \left[1 + v_2 \cos \left(\frac{2\pi}{\Lambda_2} z + c_2 \frac{z^2}{L^2} + \varphi_2 \right) \right]$$

If the two gratings have the same modulation amplitude δn and chirp value c , then a linear chirped moiré fiber grating is formed. The refractive index change is simplified to

(3)

$$\delta n_{co}(z) = 2\delta n \cos \left(\frac{2\pi}{\Lambda_c} z + \frac{\varphi_2 - \varphi_1}{2} \right) \cdot \cos \left(\frac{2\pi}{\Lambda_s} z + c \frac{z^2}{L^2} + \frac{\varphi_2 + \varphi_1}{2} \right)$$

where $\Lambda_c = 2\Lambda_1\Lambda_2/(\Lambda_1 - \Lambda_2)$, $\Lambda_s = 2\Lambda_1\Lambda_2/(\Lambda_1 + \Lambda_2)$, and $\Lambda_1 > \Lambda_2$. The difference between Λ_1 and Λ_2 is tiny, so $\Lambda_c \gg \Lambda_s$. From (3), we know that the refractive index change contains two parts, the slowly varying envelope (period Λ_c) and the rapidly varying component (period Λ_s). When the slowly varying cosine function along the z axis is equal to zero, at this point the phase of the grating changes by π . That is why a narrow pass-band appears.

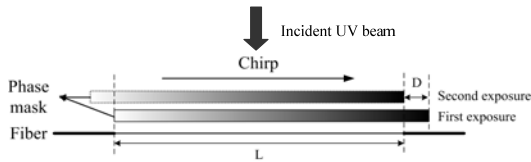


Fig. 1. Fabrication of CMFG by dual-exposure with a single chirped phase mask

According to the analysis above, CMFGs are fabricated by dual-exposure with a single chirped phase mask which is shown in Fig. 1.

The initial period difference between the two chirped gratings is described as

$$\Delta\Lambda = \Lambda_1 - \Lambda_2 = c \cdot D \quad (4)$$

where c is the chirped coefficient per unit length of the phase mask, and D is the displacement of the phase mask between the two exposures. Since the amount of the transmission peaks is related to Λ_1 and Λ_2 , we can get the amount we need by accurately controlling the displacement D . Moreover, it can be seen from (4) that the peak amount will increase if a phase mask with a larger chirped coefficient is used.

In the experiment, CMFGs with different amount of transmission peaks are fabricated by accurately tuning the displacement D . And the phase mask that is used in the experiment has a chirp value of 0.007nm/cm. The spectra of these CMFGs are shown in Fig. 2, from which we can see that, with the increase of the amount of transmission peaks, the transmittance displayed in the screen of the OSA (Optical Spectrum Analyzer) diminishes. But theoretically, the transmittance should keep invariable. That displayed result is due to the scanning resolution of the OSA. It should also be noted that the observed transmittance non-uniformity of the narrow transmission peaks of the same CMFG is on the one hand limited by the scanning resolution of the OSA, and on the other hand may be caused by the unsteadiness of exposure energy. The wavelength interval can be fine tuned by stress on the basis of need.

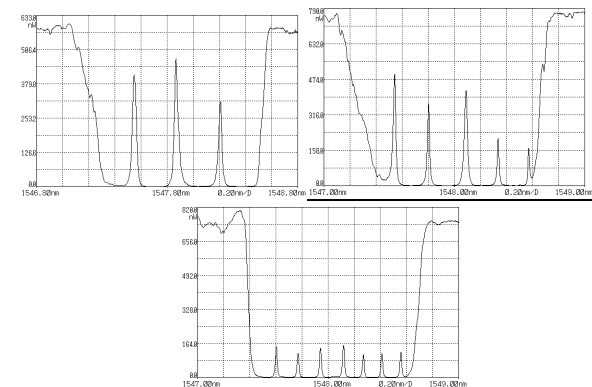


Fig. 2. Transmission spectra of CMFGs with different amounts of transmission peaks fabricated by changing the distance D

3. Principle and Laser Configuration

The schematic of the experimental setup for the proposed wavelength-switchable fiber ring laser is shown in Fig. 3. A CMFG containing five transmission peaks is incorporated in the ring cavity serving as a comb-like multichannel filter to provide periodic loss in the spectrum domain. A uniform fiber Bragg grating (UFBG) which has a reflectivity of about 99% and a narrow bandwidth of 0.07nm is utilized as the wavelength-tunable filter. As shown in Fig. 3 (a), the UFBG is usually cooperated with an optical circulator to implement its reflective property. As a low-cost substitution scheme, a fiber Sagnac loop interferometer (FSI) was recently

suggested to convert the reflective response to a transmissive response^{18, 19}. The FSI filter used here is shown in Fig. 3(b), and it consists of a 50:50 fiber coupler, a polarization controller and the UFBG. The ring cavity also comprises a 90:10 fiber coupler, an erbium-doped fiber amplifier (EDFA) and an optical isolator which provides unidirectional lasing oscillation.

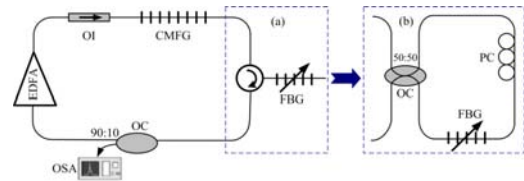


Fig. 3 Schematic of the switchable multi-wavelength fiber ring laser (a) UFBG filter containing an optical circulator (b) Sagnac loop interferometer filter

Fig. 4 displays measured the reflective spectrum of the UFBG and the transmission spectrum of the CMFG. The peak wavelength of the former can be tuned by precise temperature or strain controlling to align with one of the five peak wavelengths of the latter, and lasing will occur at the wavelength of that channel. An ANDO AQ6319 optical spectrum analyzer (OSA) with the highest resolution of 0.01nm is used to do all the measurements. It should be noted that the observed transmittance of five narrow transmission peaks of the CMFG is limited by the resolution of the OSA.

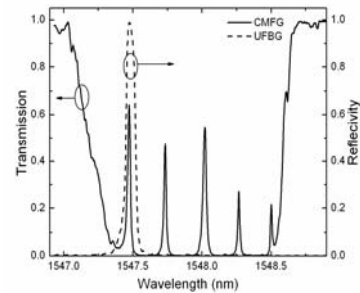


Fig. 4 Reflective spectrum of the UFBG and transmission spectrum of the CMFG

When light passes through the FSI segment, two kinds of interference will occur. Light within the UFBG resonance bandwidth is reflected from clockwise and counter-clockwise directions, and the two light beams recombine at the 50:50 fiber coupler, which result in Michelson-like interference in the spectrum of the output light. Since the path length difference of the Michelson interference is about 4m, the interference period is far less than 0.01nm which is the highest resolution of the OSA. Thus, the interference within the resonance bandwidth cannot be observed, and the transmission intensity shows a constant average value even though the polarization state is varied with the PC in the loop.

Light out of the UFBG resonance bandwidth will rotate through the UFBG and result in Sagnac interference whose period is inversely proportional to the fiber birefringence. About 5 meters commercial SMF (single mode fiber) is used in the Sagnac loop and its birefringence is at the order of 10^{-9} . According to the equation in Ref. 19, the transmission spectrum shows a broad sinusoidal period of more than 100nm, and as shown in Fig. 5 it shifts with the polarization state which is tuned by the PC resulting in different extinction ratio of the transmission peak. The highest ratio is obtained when the UFBG resonance lies in the wave trough of the periodic spectrum of the Sagnac interference. The FSI filter works at the state with the highest extinction ratio of the transmissive spectrum in Fig. 5 for lasing operation.

The variation of the FSI filter transmission along with the tuning of the UFBG is displayed in Fig.6, and it can be seen that the extinction ratio and the transmission intensity keep unchanged during the tuning process. Therefore large fluctuation among each lasing is prevented that may be caused by the transmission property change of the FSI filter.

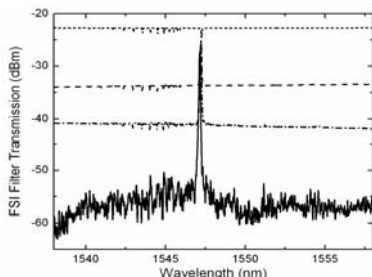


Fig.5 Transmission of the FSI filter in different polarization states

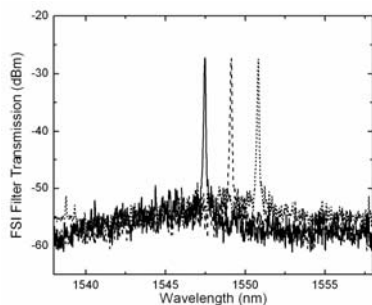


Fig.6 Transmission of FSI filter during the tuning process of the UFBG

A simple explanation of the principle of system operation may be as follows: Initially, the amplified spontaneous emission (ASE) from the EDFA passes through the CMFG which is supposed to acts as a comb filter, and the five needed in-band elements along with the extra-band light are left. Then the FSI filter will pick out one of the five elements by tuning the peak wavelength of the UFBG, and reflect most of the needed light back to the ring structure. The selected element is subsequently amplified by the EDFA. After passing through the CMFG and FSI filter, a larger portion of the selected wavelength power is reintroduced to the EDFA and reinforced. Such a process will continue until overall gain of the EDFA is equal to the loss of the cavity. In this case, a stable lasing operation can be established.

4. Experimental results and discussion

The switching result of the fiber laser is shown in Fig. 7. Lasing operation occurs at 1547.494nm, 1547.75nm, 1548.016nm, 1548.274nm and 1548.504nm corresponding to the five peak wavelengths of the CMFG. The output power difference among the five lasing oscillations is less than 1dB, and it may be caused by the inconsistent transmittance of the CMFG at each lasing wavelength which is introduced during the fabrication process of the CMFG. The extinction ratio of each laser output is as high as about 70 dB. The -3dB bandwidth of each lasing output spectrum is only ~13pm. The output power of different channels is almost identical (difference less than 1dB) within the tunable range.

16 successive scans of the system output for each lasing wavelength with a time interval of 5 seconds were carried out, and the result of lasing at 1547.75nm is recorded in Fig. 8 which indicates a good short-time wavelength stability of the laser. In order to study the long-time stability of the multi-wavelength operation at room temperature, the output

power fluctuation at each peak wavelength is measured for an hour, and it is less than 0.5dB.

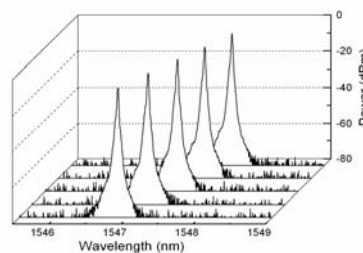


Fig.7 Individual lasing output spectrum of the fiber laser

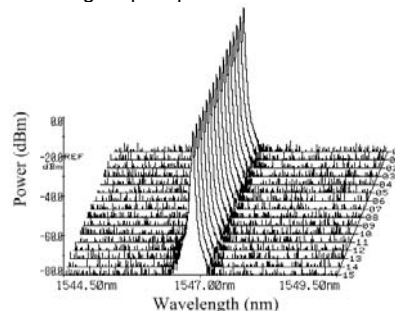


Fig.8 Lasing output spectra with 16 times repeating scans

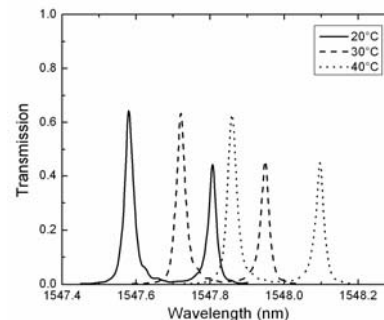


Fig.9 Transmission of CMFG at different temperature

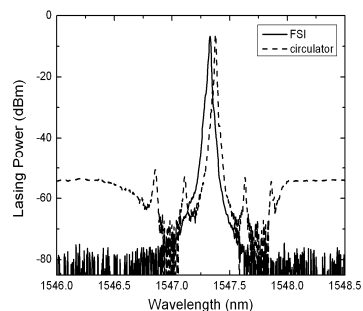


Fig.10 Lasing spectra by the FSI filter and the UFBG filter with an optical circulator

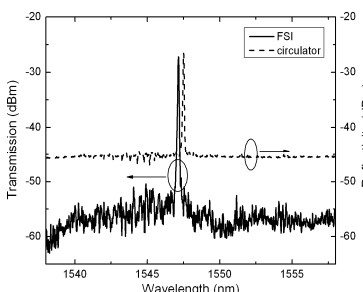


Fig.11 Transmission of the FSI filter and reflective spectrum of the UFBG with an optical circulator

We also experimentally investigated the temperature dependence of the CMFG, and for observation convenience, two of the five transmission peaks are chosen in Fig.9 to demonstrate the temperature property. The

results show that the transmission-peak wavelengths shift with the temperature simultaneously and have the same temperature coefficient as the normal FBG, and their transmittances remain unchanged. Therefore, the lasing wavelength can be fine tuned by controlling the temperature of the CFMG and the uniform FBG keeping the wavelength spacing invariant. If both the CMFG and the UFBG are tuned, the lasing wavelength can be tuned continuously over the wavelength range that the two gratings can sustain.

The usage of the FSI filter not only removes the help of a high-cost circulator, but also improves the output performance of the laser, as shown in Fig.10. The solid line represents the lasing oscillation of the laser scheme with a FSI filter in Fig.3 (b) at the wavelength of 1548.016nm, and the dashed line represents the lasing oscillation of the laser scheme with an optical circulator in Fig.3 (a) at the same wavelength. For observation convenience, the dashed curve shifts a little to the right. It is obvious that the optical signal-to-noise ratio is increased from 50 dB to 70dB. The transmission spectrum of the FSI filter and the reflective spectrum of the UFBG filter with an optical circulator are given in Fig.11, from which it can be found that light out of the UFBG resonance bandwidth are better suppressed when a FSI filter is utilized. Therefore, the high extinction ratio of the FSI filter brings the remarkable improvement of the optical signal-to-noise ratio.

In the experiment, connecting joint of every two components in the laser configuration is active FC-PC joint, and this increases the cavity loss. Replacing the active joints by splicing ones, lower threshold and higher output power can be obtained.

The phase mask with which the CMFG is fabricated has a chirp of 1nm and five transmission peaks with an interval of 0.25nm are achieved. With this phase mask, variable wavelength number and interval can be realized by precisely tuning the offset D during the process of grating fabrication, but all the transmission peaks of the CMFG are limited in the bandwidth determined by the phase mask period and the fiber parameters. More wavelengths and wavelength interval meeting the DWDM requirements are expected when using a phase mask with a higher chirp value.

5. Conclusions

We have successfully proposed and demonstrate a simple and cost-effective wavelength-switchable fiber ring laser based on a chirped moiré fiber grating (CMFG) and a wavelength-tunable Sagnac loop interferometer (FSI) filter. The CMFG possesses excellent comb-like filtering characteristics, and has extra advantages of easy fabrication and extensible channel number. The wavelength-tunable FSI filter is an ideal substitute of the grating filter containing a high-cost optical circulator, and as an additional benefit, the optical signal-to-noise ratio is remarkably improved. In summary, this laser scheme presents a simple and cost-effective solution to produce wavelength-switchable lasing oscillation at room temperature, and it has wide applications in optical sensing, optical telecommunication and instrumentation.

This work is supported by the Funding Project of Competence Development Program for Beijing VET Teachers.

REFERENCES

- [1] Feng, X.H., Liu, Y.G., Yuan, S.Z. et al., "L-Band switchable dual-wavelength erbium-doped fiber laser based on a multimode fiber Bragg grating," *Optics Express* 12 (2004) , No.16, 3834-3839
- [2] Feng, X.H., Liu, Y.G., Fu, S.G. et al., "Switchable dual-wavelength Ytterbium-doped fiber laser based on a few-mode fiber grating," *IEEE.Photon.Technol.Lett.* 16(2004), No.3, 762-764
- [3] Liu, X.M., Zhou, X.Q., Tang, X.F. et al., "Switchable and tunable multiwavelength erbium-doped fiber laser with fiber Bragg gratings and photonic crystal fiber," *IEEE.Photon.Technol.Lett.* 17(2005) , No.8, 1626-1628
- [4] Chen, D.R., Yu, Z.W., Qin, S. et al., "Switchable dual-wavelength Raman erbium-doped fibre laser," *Electron. Lett.* 42 (2006) ,No.4, 202-203
- [5] Mao, Q.H., Lit, John W.Y., "Switchable multiwavelength erbium-doped fiber laser with cascaded fiber grating cavities," *IEEE.Photon.Technol.Lett.* 14 (2002) ,No.5, 612-614
- [6] Zhao, C.L., Yang, X.F., Lu, C. et al., "Switchable multi-wavelength erbium-doped fiber lasers by using cascaded fiber Bragg gratings written in high birefringence fiber", *Opt. Commun.* 230, (2004), 313-317
- [7] Lee, Y. W. and Lee, B., "Wavelength-switchable erbium-doped fiber ring laser using spectral polarization-dependent loss element," *IEEE.Photon.Technol.Lett.* 15(2003) ,No.6, 795-797
- [8] Yang, J.L. Tjin, S. C., Ngo, N. Q. et al., "Wavelength-switchable fiber ring laser using cascaded fiber Bragg gratings combined with amplitude modulator," *Opt. Fiber Technol.* 11, (2005),361-369
- [9] Mao, Q.H., Lit, John W. Y. "L-band fiber laser with wide tuning range based on dual-wavelength optical bistability in linear overlapping grating cavities," *IEEE J. Quantum Electron.* 39(2003) ,No.10, 1252-1259
- [10] Kim, C.S., Han, Y.G., Lee, S. B. et al., "Individual switching of multi-wavelength lasing outputs based on switchable FBG filters," *Opt. Express* 15(2007) ,No.7, 3702-3707
- [11] Xiong, L.Y., Kai, G.Y., Sun, L. et al., "Dual wavelength erbium-doped fiber laser with a lateral pressure-tuned Hi-Bi fiber Bragg grating," *Chinese Opt. Lett.* 2 (2004) ,No.12, 686-687
- [12] Slavík, R., Castonguay, I., LaRochelle, S. et al., "Short multiwavelength fiber laser made of a large-band distributed Fabry-Pespl acuterot structure," *IEEE Photon. Technol. Lett.* 16(2004) ,No.4, 1017-1019
- [13] Brochu, G., LaRochelle, S. and Slavík, R., "Modeling and Experimental Demonstration of Ultracompact Multiwavelength Distributed Fabry-Pérot Fiber Lasers," *J. Lightwave Technol.* 23 (2005) ,No.1, 44-53
- [14] Liu, Y.G., Dong, X.Y., Shum, P. et al., "Stable room-temperature multi-wavelength lasing realization in ordinary erbium-doped fiber loop lasers," *Opt. Express* 14(2006) ,No.20, 9293-9298

Authors: Shaohua Lu, Beijing Vocational College of Labour and Social Security, Beijing, 100029, China, E-mail: lsh971@163.com; MeiZhang, Beijing Vocational College of Labour and Social Security, Beijing, 100029, China, E-mail: zh_mei2005@sina.com; Suchun Feng, Institute of Lightwave Technology, Beijing Jiaotong University, Beijing, 100044, China, E-mail: fengsuchun@gmail.com